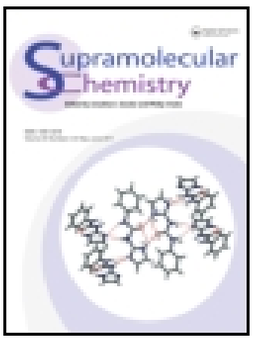

Supramolecular Chemistry

ISSN: 1061-0278 (Print) 1029-0478 (Online) Journal homepage: http://www.tandfonline.com/loi/gsch20

Colorimetric and fluorogenic anion sensors of 2'-(p-nitrophenyl)-imidazol[4',5'-f]-1,10-phenanthroline[5,6-f] and its complex of

Hua-Mei Chen , Jian-Wei Li , Hai Lin , Zun-Sheng Cai & Hua-Kuan Lin

To cite this article: Hua-Mei Chen , Jian-Wei Li , Hai Lin , Zun-Sheng Cai & Hua-Kuan Lin (2009) Colorimetric and fluorogenic anion sensors of 2′-(p-nitrophenyl)-imidazol[4′,5′-f]-1,10-phenanthroline[5,6-f] and its complex of , Supramolecular Chemistry, 21:5, 401-408, DOI: 10.1080/10610270802072785

To link to this article: https://doi.org/10.1080/10610270802072785

Published online: 30 Jun 2009.

Supramolecular Chemistry
Vol. 21, No. 5, July–August 2009, 401–408

Colorimetric and fluorogenic anion sensors of 2′-(*p*-nitrophenyl)-imidazol[4′,5′-*f*]-1,10-phenanthroline[5,6-*f*] and its complex of Ru(bipy)$_2^{2+}$

Hua-Mei Chen[a], Jian-Wei Li[a], Hai Lin[b], Zun-Sheng Cai[a] and Hua-Kuan Lin[a]*

[a]*Department of Chemistry, Nankai University, Tianjin, People's Republic of China;* [b]*Key Laboratory of Functional Polymer Materials of Ministry of Education, Nankai University, Tianjin, People's Republic of China*

(*Received 30 April 2007; final version received 17 March 2008*)

2′-(*p*-nitrophenyl)-imidazol[4′,5′-*f*]-1,10-phenanthroline[5,6-*f*] (**1**) and its Ru(bipy)$_2^{2+}$ complex (**2**) were synthesised and studied for the anion sensing by UV–vis, fluorescence and ^{1}H NMR titration experiments. Compounds **1** and **2** exhibited obviously different changes between reactions with AcO^-, F^-, $H_2PO_4^-$ and with other halogens, i.e. Cl^-, Br^-, I^-, in any of the UV–vis, fluorescence and ^{1}H NMR titration spectra in DMSO experiments. With an 89 nm red shift, **1** was convenient to be employed to detect anions with the naked eye. Complexed with the electron withdrawing metal ion, **2** had the stronger interaction with anions to be detected than **1** had.

Keywords: anion sensor; colorimetry; fluorescence; ^{1}H NMR; Ru(bipy)$_2^{2+}$; X-ray structure

Introduction

In the last decade, the development of synthetic sensors for anions has attracted considerable attention within the field of supramolecular chemistry due to the fact that a large number of biological processes involve the recognition of anionic species (*1–3*). Among the various kinds of mechanisms of anion sensing, selective colorimetric anion sensing is particularly challenging since visual detection can immediately give qualitative information, although absorption spectroscopy gives quantitative information. Generally, most of the colorimetric anion sensors contain the chromophore that is covalently attached to the anion recognition unit (*4*). We have recently found that imidazole (*5–7*) and imidazolium compounds (*8*) used as important fragments in anion sensors present selectivity on the recognising anions. This result should be associated with several factors. First, the NH of imidazole equipped with anthraquinone or phenyl is active and is generally highly acidic as indicated naturally by its relatively high chemical shift in the range of 13–15 ppm. In addition, the acidity of benzimidazole is also strong [pK_a = 16.4 in dimethyl sulphoxide (DMSO)] (*9*). Moreover, various types of special arrangement of imidazolium rings on suitable spacers have produced tweezer-type (*10*), tripodal (*11, 12*) and cyclic imidazolium receptors (*13–15*), which utilised the C(2)—H in the imidazolium ring to form strong $(C—H)^+\cdots X^-$ hydrogen bonds with the anion X^-. A number of sensors incorporating transition metal complexes of 2,2′-bipyridyl (*16–18*), ferrocene (*19, 20*) or cobaltocenium (*21*) were also prepared and studied. However, to our knowledge, the receptors bearing imidazolium and 1,10-phenanthroline or its complex have been hardly reported so far.

In this paper, we present the colorimetric and fluorescence sensors of anions, i.e. 2′-(*p*-nitrophenyl)-imidazol[4′,5′-*f*]-1,10-phenanthroline[5,6-*f*] (**1**) and its complex of $[Ru(bipy)_2]^{2+}$ (**2**). Compound **1** comprises a chromophore of *p*-nitrophenyl and **2** comprises a photoactive Ru(bipy)$_2$ moiety (bipy = 2,2′-bipyridine) besides the same chromophore group. The existence of a photoactive Ru–bipy unit not only enhances the affinity due to the electrostatic interactions but also provides the fluorogenic property. Compounds **1** and **2** can be considered as a kind of a poor receptor for Cl^-, Br^- and I^-, but the proton of NH can be transferred to AcO^-, $H_2PO_4^-$ and F^- and at the same time a potential hydrogen bond with C—H of phenyl can be formed making it a good receptor for these three anions.

Experimental

Materials and instruments

All common chemicals were of analytical grade and were available commercially. DMSO was dried with CaH_2 for about 24 h and distilled at reduced pressure. All tetrabutylammonium salts were dried for 24 h in vacuum with P_2O_5 at 353 K before use. 5,6-Diamino-1,10-phenanthroline (*22*) and $[Ru(bipy)_2Cl_2]\cdot 2H_2O$ (*23*) were synthesised according to the previous literatures.

*Corresponding author. Email: hklin@nankai.edu.cn

ISSN 1061-0278 print/ISSN 1029-0478 online

DOI: 10.1080/10610270802072785
http://www.informaworld.com

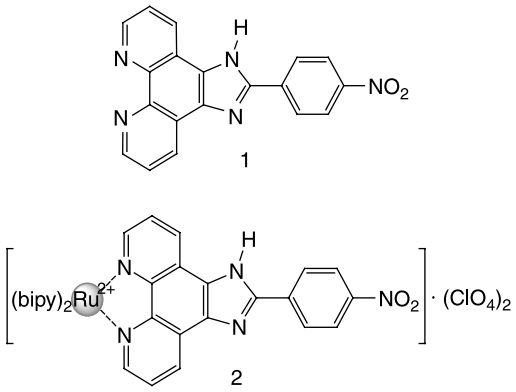

Scheme 1. Molecular structure of the sensors **1** and **2**.

UV–vis and fluorescence spectra were recorded on SHIMADZU 2450 with TCC-240A controller and RF-5301. ^{1}H NMR spectra were obtained using a Varian UNITY Plus-400 MHz unit, operating at room temperature. C, H, N elemental analyses were made on Elementar vario EL. ESI-MS was performed with a MARINER apparatus. The crystal structures were measured on a Rigaku Saturn CCD.

*Synthesis of 2′-(***p***-nitrophenyl)-imidazol[4′,5′-***f***]-1, 10-phenanthroline[5,6-***f***] (1)*

The synthesis of **1** and **2** is outlined in Scheme 1. 5,6-diamino-1,10-phenanthroline (210 mg, 1.0 mmol) and 4-nitrobenzaldehyde (1.0 mmol) were refluxed in 15 ml dry ethanol for 36 h. After cooling, the precipitate was filtered as a dirty yellow powder; yield 80%. ^{1}H NMR (DMSO-d_6): 14.119 (s, 1H, NH), 9.065 (s, 2H, phen-H), 8.917–8.937 (tri, 2H, phen-H), 8.478–8.537 (dd, 4H, Ar-H), 7.889–7.909 (tri, 1H, phen-H), 7.823–7.877 (tert, 1H, phen-H). ESI-MS: *m*/*z* 341.1. Calcd for $C_{19}H_{11}N_5O_2{\cdot}0.25H_2O$: C, 65.93; H, 3.33; N, 20.24. Found: C, 66.03; H, 3.38; N, 19.80 (Scheme 2).

Synthesis of [Ru(bipy)$_2$(1)](ClO$_4$)$_2$·H$_2$O (2)

Compound **2** was synthesised following the literature procedure (*24*); yield 85%. ^{1}H NMR (DMSO-d_6): 7.360 (s, 2H, bipy), 7.623 (s, 4H, bipy-H), 7.858, 7.948 (d, 4H, phen-H), 8.100 (s, 4H, bipy-H), 8.226 (s, 2H, bipy-H), 8.520, 8.550 (d, 4H, Ar-H), 8.872 (s, 4H, bipy-H), 9.101 (s, 2H, phen-H), 14.714 (br, 1H, NH). ESI-MS: *m*/*z* 754.4 (M-ClO$_4$), 853.96 (M-2ClO$_4$). Calcd for [Ru(bipy)$_2$(**1**)](ClO$_4$)$_2$·H$_2$O ($C_{39}H_{29}Cl_2N_9O_{11}Ru$): C, 48.21; H, 3.01; N, 12.97; found: C, 48.12; H, 3.07; N, 12.94.

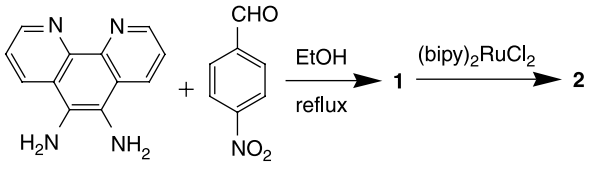

Scheme 2. Synthesis of sensors **1** and **2**.

Crystal data and structure determination

A red bulk-like crystal of $C_{41}H_{27}Cl_2N_9O_{15.5}Ru$ having approximate dimensions of 0.24 × 0.25 × 0.18 mm was mounted on a glass fibre. All measurements were performed on a Rigaku Saturn CCD area detector with graphite monochromated Mo K radiation. The data were collected at a temperature of 294 ± 1 K. A sweep of data was done using ω scans. Out of the 13,535 reflections that were collected, 9644 were unique ($R_{int} = 0.0651$). Data were collected and processed using CrystalClear (Rigaku). The structure was solved by direct methods and expanded using Fourier techniques. The non-hydrogen atoms were refined anisotropically. Hydrogen atoms were refined using the riding model. The final cycle of full-matrix least-squares refinement on F^2 was based on 9644 observed reflections and 581 variable parameters and converged with unweighted and weighted agreement factors of $R_1 = 0.1146$, $wR_2 = 0.2516$. The SD of an observation of unit weight was 1.115. Unit weights were used. All calculations were performed using the CrystalStructure crystallographic software package except for refinement, which was performed using SHELXL-97 (*25*). Selected bond lengths and angles are summarised in Table 1.

After many attempts, the crystal measured (in this paper) is relatively the best quality one which we have obtained. The red crystals are sharp prisms in the mother liquid; however, once the crystals are taken out from the mother liquid they became slim very soon. As a result, after the solvent was removed, the crystal (in this paper) can be barely stable for a long time. Therefore, it cannot persist in the measurement for collecting enough good data. Finally, the instability of the crystal quality resulted in a shift by 0.012. The partial occupancy by chloride ions was used to take the place of OH and H_2O and keep the complex electrically neutral. As a limitation of the quality of the crystal, the structure of the part of the solvent cannot be determined absolutely; however, the part of the metal and ligands are determined correctly.

CCDC reference number 615438.

Results and discussion

UV–vis titration studies

The UV–vis titration experiments were carried out in DMSO solution. With the addition of AcO^- (Figure 1(a)) to the solution of sensor **1**, the absorption peak at 386 nm decreased and two new peaks at 315 and 476 nm appeared

Table 1. Log K[a] for **1** and **2** interacting[on] with anions in DMSO solution 298.2 ± 0.1 K.

	AcO^-	OH^-	$H_2PO_4^-$	F^-	Cl^-	Br^-	I^-
1	> 6	> 6	4.65 ± 0.1	4.15 ± 0.1	2.04 ± 0.2	1.20 ± 0.1	–[b]
2	> 6	> 6	5.97 ± 0.2	5.20 ± 0.2	2.80 ± 0.1	1.75 ± 0.2	–[b]

[a] Determined by UV–vis spectroscopy.
[b] Very weak change in spectra. Binding constant cannot be determined.

gradually accompanying the formation of three clear isoabsorptive points at 291, 335 and 424 nm, respectively. The spectra of the receptor **1** changed, similar to those when AcO^- was added, after titrating with $H_2PO_4^-$ and F^-. Furthermore, the solution of receptor **1** had a remarkable colour change from yellow to red with the order of the significance $AcO^- > H_2PO_4^- > F^-$. On the contrary, after the Cl^-, Br^- and I^- were added to the solution of receptor **1**, respectively, the colour did not change. These colour changes are well representing the changes in the spectra.

When excess Cl^- was added further from 250 up to 2900 equiv (Figure 1(b)), the peak at 388 nm decreased and the peak at 332 nm developed with the association constant $\log K = 2.04$. It can be seen that the spectra are distinctly different from those in Figure 1(a).

With the addition of AcO^- to the solution of **2** (Figure 2(a)), the absorption at 364 nm decreased and the band centred at 460 nm increased with a red shift of 8 nm. Naturally, three clear isoabsorptive points appeared at 317, 338 and 396 nm, respectively. $H_2PO_4^-$, F^- also induced the changes in the spectra of **2** similar to those obtained by the addition of AcO^-.

While the spectra for **2** after the addition of Cl^- (Figure 2(b)) were different from those obtained after the addition of AcO^-, $H_2PO_4^-$ and F^-, the band from 350 to 500 nm decreased and a little trough at 325 nm developed with an isoabsorptive point at 346 nm, which reflects that the interaction between **2** and Cl^- is visibly different from that of with AcO^-, $H_2PO_4^-$ and F^-. Additionally, the analogous UV–vis titration experiments with the

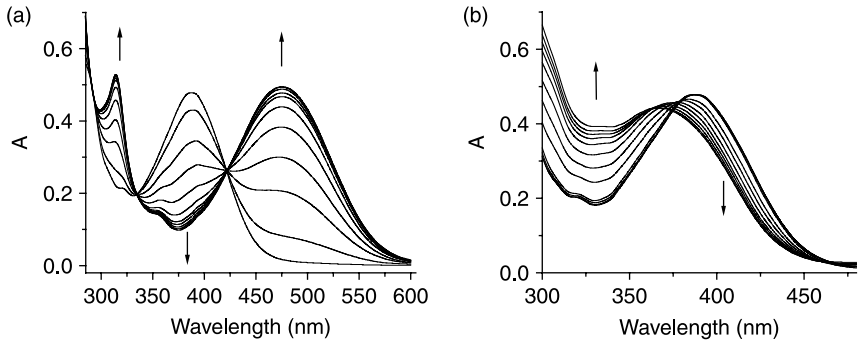

Figure 1. Changes in the absorption spectra for **1** (2×10^{-5} M) in DMSO with the addition of (a) 0–3 × 10^{-4} M $[(Bu)_4N]AcO$ and (b) 0–6 × 10^{-2} M $[(Bu)_4N]Cl$ at 298.2 ± 0.1 K.

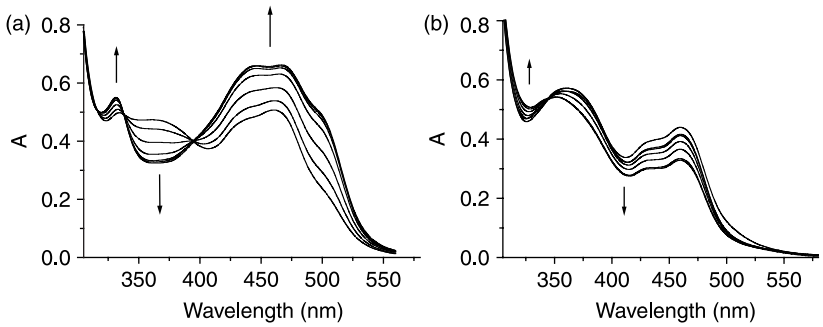

Figure 2. Changes in the absorption spectra for **2** (2×10^{-5} M) in DMSO with the addition of (a) 0–5 × 10^{-4} M $[(Bu)_4N]AcO$ and (b) 0–8 × 10^{-2} M $[(Bu)_4N]Cl$ at 298.2 ± 0.1 K.

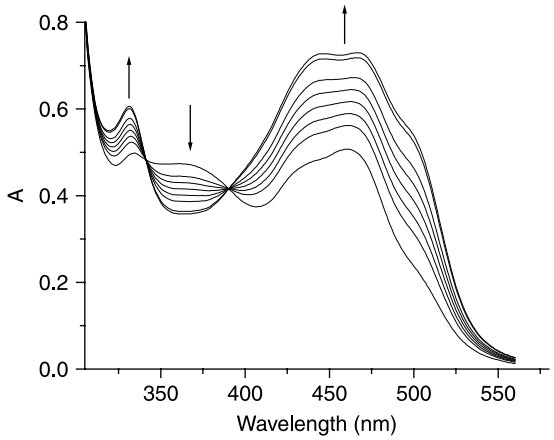

Figure 3. Changes in the absorption spectra for **2** (2×10^{-5} M) in DMSO with the addition of 0–3.5×10^{-4} M $[(Bu)_4N]OH$ at 298.2 ± 0.1 K.

base, i.e. hydroxide, were also carried out, and the spectral changes were similar to those obtained after the addition of AcO^-, $H_2PO_4^-$ and F^- (Figure 3), and the anion affinity of receptor **2** varied in the order of AcO^-, $OH^- > H_2PO_4^- > F^- \gg Cl^- > Br^-$, I^-.

Fluorescence titration studies

To learn more about the properties of **1** and **2** as anion receptors, fluorescence titration was performed. In DMSO solution, **1** has a strong luminescence at 566 nm, when excited at 387 nm. However, it is quenched by the titration of all the investigated anions (Figure 4), i.e. AcO^-, $H_2PO_4^-$, F^-, Cl^-, Br^- and I^-. With the addition of F^-, the luminescence is extinguished quickly (Figure 4(a)). On the other hand, when Cl^- was titrated with the solution of **1**, the quenching was very slow with the peak shifting from 566 to 558 nm (Figure 4(b)), forming an isoabsorptive point at 515 nm.

The fluorescence of **2** was enhanced by AcO^-, $H_2PO_4^-$ and F^- (Figure 5(a)) but quenched by Cl^-, Br^- and I^- (Figure 5(b)). In DMSO solution, compound **2** was excited at 468 nm and then emitted at 523 and 610 nm. With the titration of AcO^- to a solution of **2**, the peak at 619 nm developed dramatically with a shift to 623 nm but the peak at 521 nm decreased slightly. On the other hand, the change is opposite to that found in Figure 5(a) after the addition of Cl^- to the solution (Figure 5(b)). The peak at 523 nm was enhanced and the peak at 610 nm quenched. Sensors **1** and **2** undergo the excited state intermolecular proton transfer, which makes a contribution to their deprotonation after the addition of AcO^-, $H_2PO_4^-$ and F^- (*3a*).

Both UV–vis and fluorescence spectra show two different kinds of changes between the addition of AcO^-, $H_2PO_4^-$, F^- and that of Cl^-, Br^-, I^-, which suggests that the interaction of sensors **1** and **2** with the studied anions belongs to two different mechanisms.

Table 1 shows the apparent affinity constants for **1** and **2** with anions by fitting the UV–vis titration data. In addition, all of the obtained apparent affinity constants for **1** are smaller than those for **2**. Because Ru^{2+} draws electron from ligand **1**, the electron density on N of HN of the imidazol is decreased and the acidity of HN of the imidazol increased. Also, it may be seen from the ^1H NMR of **2** that the signal of NH is at 14.714 ppm and as a broad signal, which is away from the signal of NH of **1** at 14.19 ppm. The acidity of NH results in the affinity constants of sensor **2** with anions larger than that of sensor **1**.

^1H NMR titration studies

To this system, further investigations of the insights into the nature of sensor–anion interaction were carried out by the analysis of ^1H NMR spectra. Figure 6 displays the spectra for ^1H NMR titration of **1** with Cl^- and F^-. Figure 6(a) shows the adscription of the protons of sensor **1**. From Figure 6(b), the spectra of **1** titration with Cl^-, the signals of NH, $H_{cc'}$ and $H_{11'}$ have gone

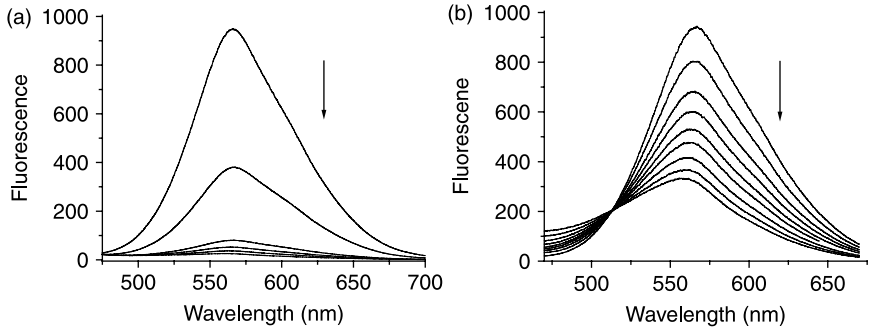

Figure 4. Changes in the fluorescence spectra for **1** (2×10^{-5} M) in DMSO with the addition of (a) 0–3×10^{-4} M $[(Bu)_4N]AcO$ and (b) 0–5×10^{-2} M $[(Bu)_4N]Cl$ at 298.2 ± 0.1 K.

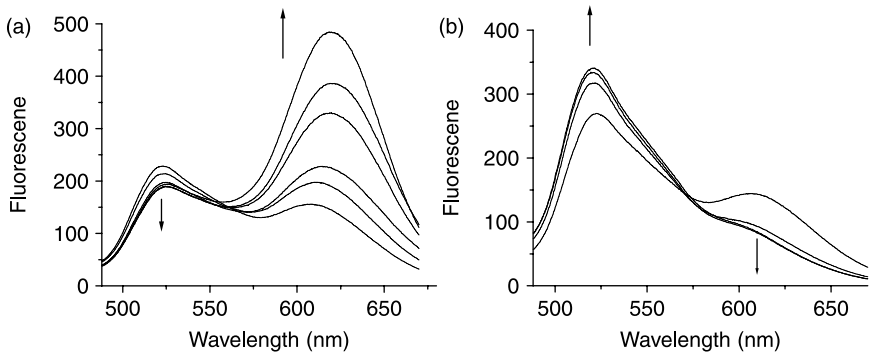

Figure 5. Changes in the fluorescence spectra for **2** (2×10^{-5} M) in DMSO with the addition of (a) $0-4 \times 10^{-5}$ M $[(Bu)_4N]AcO$ and (b) $0-2 \times 10^{-3}$ M $[(Bu)_4N]Cl$ at 298.2 ± 0.1 K.

to downfield, which suggests that the hydrogen bond complex is formed. As it can be seen from Figure 6(a), $H_{cc'}$ and $H_{11'}$ are near the predictable binding site of imidazole NH; hence they are unavoidably involved in the receptor–anion complex formation and affected during the receptor–anion complex formation through polarisation and electrostatic repulsion interaction.

The electron density on the receptor decreased, especially on NH and $H_{c'}$, which produced a deshielded effect after which the signals moved downfield. The hydrogen bond of the complex formed at the side of the receptor plane with $H_{c'}$, therefore the signal of $H_{cc'}$, divided into two separate signals with an obvious downfield shift of $H_{c'}$.

With the addition of F^- (Figure 6(c)), the signals of general C—H exhibited upfield shifts, whereas the signal of $H_{11'}$ exhibited a downfield shift. The promotion of the downfield shift suggests that the complexed anion

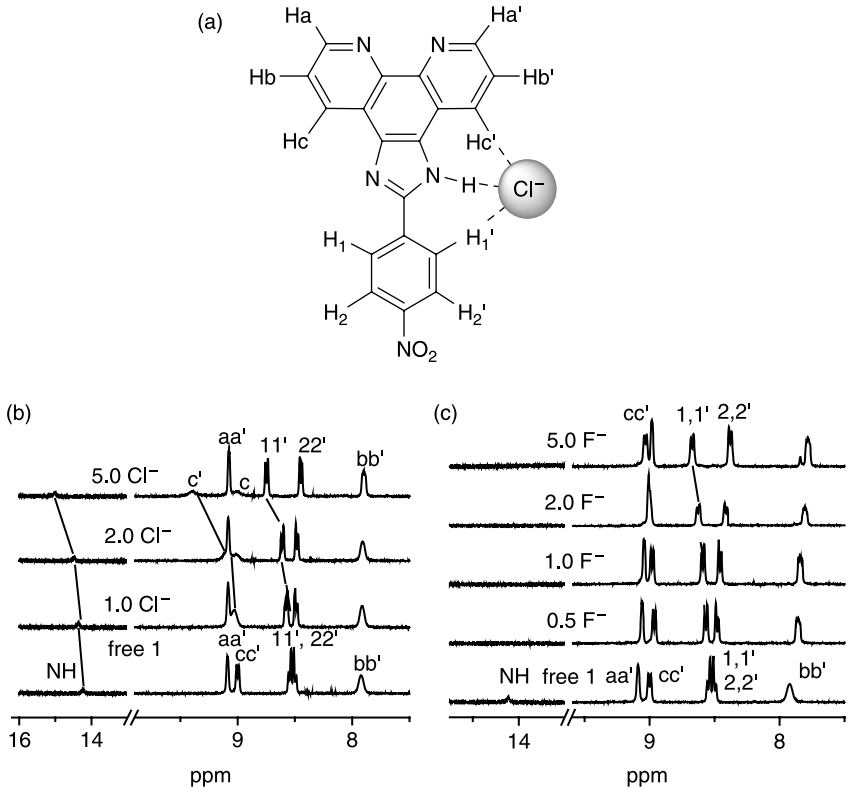

Figure 6. (a) The proposed binding made between 1 and Cl^-; ^1H NMR titration of **1** (5×10^{-3}) with (b) $[(Bu)_4N]Cl$ and (c) $[(Bu)_4N]F$ in DMSO-d_6.

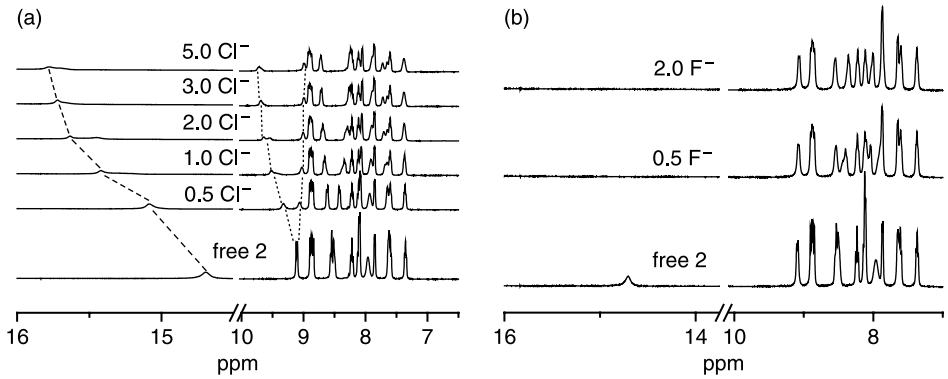

Figure 7. ^{1}H NMR titration of **2** (5×10^{-3} M) with (a) $[(Bu)_4N]Cl$ and (b) $[(Bu)_4N]F$ in DMSO-d_6.

is positioned near $H_{11'}$ (*26*), while the general C—H signals that have gone upfield indicate that the deprotonation on the imidazole.

Similarly, the proton NMR titration experiments were performed between **2** and anion Cl^- or F^- (Figure 7). And the results revealed that the interaction between them was similar to that of receptor **1**. The complex was formed by **2** binding the anion Cl^- definitely; however, F^- induced the same amount of deprotonation with even a less amount of titration of F^-.

In summary, the mechanism of sensor **1** responding with AcO^-, F^- and $H_2PO_4^-$ is by deprotonation and by forming a potential hydrogen bond with $H_{11'}$. However, Cl^-, Br^- and I^- form a hydrogen bond with NH, $H_{c'}$ and $H_{1'}$. And, in all of the cases, the mechanism of the receptor of Ru^{2+} complex **2** is the same as that of **1**.

X-ray structure of Ru^{2+} complex (2)

Red prism crystals of complexes of **2** were formed in the solvent mixture of CH_3CN and CH_3OH in several days, but once the crystal is taken out of the mother liquid it becomes a dope. The possible cause for this could be that the solvents CH_3CN and CH_3OH covering and/or in the prism are easy volatile, which induces the framework of the crystal to be collapsed by air and/or moisture. Hence, another attempt was made to use the mixture of ethanol and DMF, which is less volatile relatively. Red single crystals of the complexes of **2** suitable for X-ray diffraction studies were grown from slow evaporation of the solution of **2** in solvent mixture of CH_3CH_2OH and DMF for the second time. As expected, the crystal is a little more stable than that was formed in CH_3CN and CH_3OH. Not satisfied, however, during the X-ray measurement bulk of the crystal mounted on the machine is effloresced, which leads to the data collected with poor quality relatively. Therefore, other attempts were performed until the data are suitable for structural analysis. In the process of refinement, the coordinates of the solvent cannot be determined from the poor data. Another reason is that the number of solvent molecules in the crystal is always in varying, which caused a great difficulty in the refinement of the solvent coordinates. The crystal data and selective bond lengths and angles are listed in Tables 2 and 3, respectively.

The molecular structure of **2** consists of a $[Ru(bipy)_2(\mathbf{1})]^{2+}$ cation, a disordered ClO_4^-, a Cl^-, an ethanol and 5.5 H_2O molecule. A ball and stick drawing of the cation with selected atomic numbering scheme is shown in Figure 8.

Table 2. Crystal data collection and refinement details for **2**.

Formula	$C_{41}H_{27}Cl_2N_9O_{15.5}Ru$	γ (°)	85.480(4)
Molecular weight	1065.69	V (Å^3)	2374.9(8)
Colour	Red block	Z	2
Dimension (mm)	$0.25 \times 0.24 \times 0.18$	D (calc)/g/cm^3	1.490
Crystal system	Triclinic	Measured reflns	13,534
Space group	*P*-1	Unique reflns	9643
a (Å)	8.4046 (17)	R_{int}	0.0651
b (Å)	16.106 (3)	Strong data [$I_o > 2\sigma(I_o)$]	3858
c (Å)	18.420 (4)	R_1 (strong data)	0.1146
α (°)	74.499 (4)	R, wR_2 (all data)	0.2516, 0.3769
β (°)	81.604 (4)	GOF	1.029

Table 3. Selected bond lengths (Å) and angles(°) for **2**.

Ru(1)—N(1)	2.054(9)	Ru(1)—N(4)	2.035(12)
Ru(1)—N(2)	2.086(11)	Ru(1)—N(5)	2.064(9)
Ru(1)—N(3)	2.045(11)	Ru(1)—N(6)	2.066(9)
N(8)—C(33)	1.340(16)	N(8)—C(26)	1.348(14)
N(7)—C(33)	1.318(15)	N(7)—C(25)	1.378(15)
N(1)—Ru(1)—N(2)	77.8(4)	N(1)—Ru(1)—N(5)	98.5(3)
N(3)—Ru(1)—N(4)	77.9(5)	N(2)—Ru(1)—N(3)	89.3(4)
N(5)—Ru(1)—N(6)	79.9(3)	N(2)—Ru(1)—N(4)	96.8(5)
N(1)—Ru(1)—N(3)	96.2(5)	N(2)—Ru(1)—N(5)	174.1(4)
N(1)—Ru(1)—N(4)	172.2(5)	N(4)—Ru(1)—N(5)	87.3(4)
N(1)—Ru(1)—N(6)	87.5(3)	N(4)—Ru(1)—N(6)	98.8(4)
N(2)—Ru(1)—N(6)	95.3(4)	N(3)—Ru(1)—N(5)	95.7(4)
N(3)—Ru(1)—N(6)	174.7(4)	C(33)—N(7)—C(25)	102.6(10)
C(33)—N(8)—C(26)	108.0(10)		

As shown in Figure 8, the central Ru^{2+} atom is chelated by two bipy ligands and a **1** ligand. The average Ru—N bond length of 2.058 Å is comparable with that published for $[Ru(phen)_3]^{2+}$(2.063 Å) (*27*), although there are some differences in the size and shape among phen, bipy, and **1**. The coordination geometry around the Ru^{2+} atom is that of a distorted octahedron, with a bite angle of 78.5° averaged over the three bidentate ligands. Of most interest is the configuration of the ligand **1** in the complex. To minimise the possible electrostatic interaction between the H atom in the nitrophenyl and the imidazole ring, the nitrophenyl group is slightly twisted with respect to the imidazo[4′,5′-*f*]-1,10-phenanthroline[5,6-*f*] plane forming a dihedral angle of 4.8°. And the formation of the hydrogen bond between H—N of imidazole group and ClO_4^- is the existing reason for the distance between H—N of imidazole and one oxygen atom of O(17) in ClO_4^-: the distance of (N(8)—H(8A)—O(17)) is 2.74(2) Å. It indicates the H—N of imidazole group to be a recognition site.

From Figure 9 we can see that there exists π–π stacking between the two **1** ligands of the Ru^{2+} complex, and the distance between the two planes is 3.56(6) Å.

Conclusion

Two new receptors, 2′-(*p*-nitrophenyl)imidazol[4′,5′-*f*]-1,10-phenanthroline (**1**) and its Ru(α) complex (**2**), with imidazole group as the recognition site and nitrophenyl groups as the chromophore were designed and synthesised. UV–vis and fluorescence titration experiments show that the two receptors have a high sensitivity towards the AcO^-, $H_2PO_4^-$ and F^- with a decreasing trend: $AcO^- > H_2PO_4^- > F^-$, while with little sense to Cl^-, Br^-, I^-. Particularly, **1** has a remarkable colour change, and hence it is convenient to detect the anion

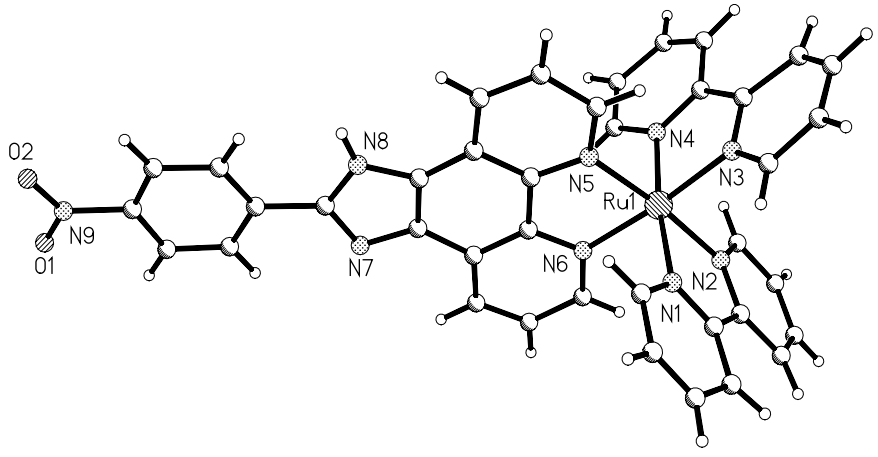

Figure 8. The coordination environment of the Ru^{2+} complex.

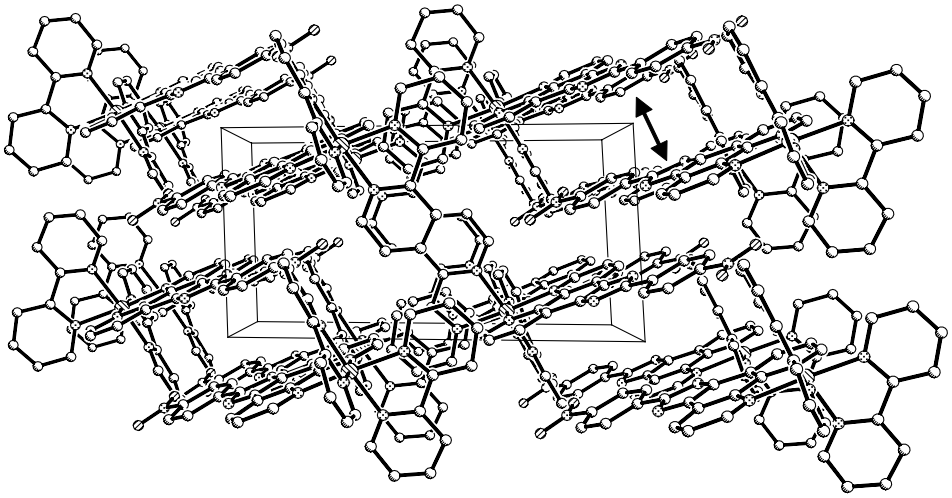

Figure 9. The π−π stacking in the crystal formed from overlapping sections of the aromatic ligands.

with it by naked eye. The sensors have form a hydrogen bonded supramolecular complex with Cl^- and Br^-, and are transferring proton to AcO^-, F^- $H_2PO_4^-$, then forming potential hydrogen bond with C—H of the phenyl.

Acknowledgements

This work was supported by the National Natural Science Foundation of China (Nos. 20371028, 20671052) and the Natural Science Foundation of Tianjin of China (No. 023605811).

References

(1) Stibor, I. *Anion Sensing Top. Curr. Chem.* **2005**, *255*.
(2) Best, M.D.; Tobey, S.L.; Anslyn, E.V. *Coord. Chem. Rev.* **2003**, *240*, 3–15.
(3) Bondy, C.R.; Loeb, S.J. *Coord. Chem. Rev.* **2003**, *240*, 77–99.
(4) Ramón, M.M.; Félix, S. *Chem. Rev.* **2003**, *103*, 4419–4476.
(5) Peng, X.-J.; Wu, Y.-K.; Fan, J.-L.; Tian, M.-Z.; Han, K.-L. *J. Org. Chem.* **2005**, *70*, 10524–10531.
(6) Kang, J.-M.; Kim, H.-S.; Jang, D.-O. *Tetrahedron Lett.* **2005**, *46*, 6079–6082.
(7) Ion, L.; Morales, D.; Pérez, J.; Riera, L.; Riera, V.; Kowenicki, R.-A.; McPartlin, M. *Chem. Commun.* **2006**, 91–93.
(8) Chellappan, K.; Singh, N.J.; Hwang, I.C.; Lee, J.W.; Kim, K.S. *Angew. Chem. Int. Ed.* **2005**, *44*, 2899–2903.
(9) Bordwell, F.G. *Acc. Chem. Res.* **1988**, *21*, 456–463.
(10) Kim, S.K.; Singh, N.J.; Kim, S.J.; Kim, H.G.; Kim, J.K.; Lee, J.W.; Kim, K.S.; Yoon, J. *Org. Lett.* **2003**, *5*, 2083–2086.
(11) Yun, S.; Ihm, H.; Kim, H.G.; Lee, C.W.; Indrajit, B.; Oh, K.S.; Gong, Y.J.; Lee, J.W.; Yoon, J.; Lee, H.C.; Kim, K.S. *J. Org. Chem.* **2003**, *68*, 2467–2470.
(12) Ihm, H.; Yun, S.; Kim, H.G.; Kim, J.K.; Kim, K.S. *Org. Lett.* **2002**, *4*, 2897–2900.
(13) Yoon, J.; Kim, S.K.; Singh, N.J.; Lee, J.W.; Yang, Y.J.; Chellappan, K.; Kim, K.S. *J. Org. Chem.* **2004**, *69*, 581–583.
(14) Beer, P.D.; Hayes, E.J. *Coord. Chem. Rev.* **2003**, *240*, 167–189.
(15) Mizuno, T.; Wei, W.H.; Eller, L.R.; Sessler, J.L. *J. Am. Chem. Soc.* **2001**, *124*, 1134–1135.
(16) Evans, A.J.; Matthews, S.E.; Cowley, A.R.; Beer, P.D. *Dalton Trans.* **2003**, *46*, 4644–4650.
(17) Thomas, J.L.; Howarth, J.; Hanlon, K.; Guirk, D.M. *Tetrahedron Lett.* **2000**, *41*, 413–416.
(18) Miyaji, H.; Collinson, S.R.; Prokeŝ, I.; Tucker, J.H.R. *Chem. Commun.* **2003**, 64–65.
(19) Beer, P.D.; Drew, M.G.B.; Hesek, D.; Nam, K.C. *Chem. Commun.* **1997**, 107–108.
(20) Beer, P.D.; Hesek, D.; Nam, K.C.; Drew, M.G.B. *Organometallics* **1999**, *18*, 3933–3943.
(21) Kang, S.K.; Llinares, J.M.; Powell, D.; Velde, V.; James, B. *J. Am. Chem. Soc.* **2003**, *125*, 10152–10153.
(22) Bodige, S.; MacDonnell, F.M. *Tetrahedron Lett.* **1997**, *38*, 8159–8160.
(23) Sullivan, B.P.; Salmon, J.; Meyer, T.J. *Inorg. Chem.* **1978**, *17*, 3334–3341.
(24) Liu, J.-G.; Ye, B.-H.; Li, H.; Zhen, Q.-X.; Ji, L.-N.; Fu, Y.-H. *J. Inorg. Chem.* **1999**, *76*, 265–271.
(25) Sheldrick, G.M. SHELXS97 and SHELXL97; University of Gŏttingen, Germany, **1997**.
(26) Shionoya, M.; Furuta, H.; Lynch, V.; Harriman, A.; Sessler, J.L. *J. Am. Chem. Soc.* **1992**, *114*, 5714–5722.
(27) Bueu, J.; Stoll, A. *J. Acta Crystallogr. Sect. C* **1996**, *52*, 1174.